5
Charge Trapping Dynamics

The charge trapping in organic field-effect devices is investigated with the help of displacement current measurements. The long-channel capacitor (LCC) structure was fabricated for performing these measurements. From the displacement currents, the number of charges injected into and extracted from the semiconductor and the density of charges trapped in the device during each measurement is calculated for evaluating and comparing the charge-carrier dynamics of devices with different organic semiconductors and metal contacts.

5.1 INTRODUCTION

Organic TFTs have a thin layer of conjugated organic molecules, as a semiconducting active layer. The principle of operation is to some extent similar to that of silicon MOSFETs. In both devices, the magnitude of the electric current flowing through the semiconductor is controlled by the gate field and can be, to first order, described by the same formalism [Marinov *et al*, 2009]. The physical mechanisms, however, are notably different.

For example, the charge-carrier channel in a silicon MOSFET is formed by the inversion of the doped semiconductor near the gate-dielectric interface, *i.e.*, the charge-carriers forming the channel originate from the semiconductor, and they remain in the semiconductor when the channel is switched off. In contrast, organic semiconductors usually have vanishingly small carrier densities, so the formation of a channel in the semiconductor requires the injection of the necessary charges from the source/drain contacts, and when the channel is removed, the charges are extracted through the contacts. This makes it possible to directly measure the number of charges forming the accumulation channel and the number of charges released during channel annihilation. The difference of the number of accumulated charges and released charges during annihilation gives the number of charges being trapped into localized electronic states in the devices. Since charge-carrier trapping during device operation has a significant influence on the device reliability [Sirringhaus, 2009; Bobbert *et al*, 2012], a better quantitative understanding of the trapping dynamics in organic TFTs is of substantial interest.

As already discussed in Chapter 4, the location of these localized electronic states (defects) is very illusive and hugely dependent on the organic semiconductor and dielectric materials used in the devices, and the interfaces formed between them. To look into this issue, LCC devices were fabricated in this work, to study the effect of using different organic semiconductors on the density of trapped charge-carriers using DCM technique. To consider the change in density of trapped charge-carriers only due to use of different organic semiconductors, the LCC devices were fabricated on same dielectric treated with SAM to improve the interface between the semiconductor and dielectric. In addition, LCC devices were fabricated using four different metal contacts having different contact barriers with one particular semiconductor to study the effect of using different metal contacts on the density of trapped charge-carriers in devices using DCM technique.

5.2 DISPLACEMENT CURRENT MEASUREMENT

A particularly useful method for studying the charge trapping dynamics is DCM, which was first introduced to organic TFTs by Ogawa *et al* [Ogawa *et al*, 2003; Ogawa 2005; Ogawa *et al* 2005; 2006; 2007] and later substantially extended by the group of Dan Frisbie [Xia *et al*, 2007; Liang *et al*, 2009; Chang *et al*, 2010; 2011; Liang *et al*, 2011]. In the DCM method, the transistor is biased like a metal-insulator-semiconductor capacitor, *i.e.*, a voltage that slowly changes in magnitude, is applied between the gate electrode and a metal contact that is in direct contact with the semiconductor. This time-dependent change of the applied voltage causes a displacement current to flow into the semiconductor through the metal contact during forward sweep and a displacement current to flow out of the semiconductor through the metal contact during reverse sweep. This displacement current is continuously measured at the contact. In principle, a DCM configuration with two metal contacts (source and drain, as in a transistor) is also feasible. In this case, the measurement can be conducted either by shorting the two contacts [Ogawa *et al*, 2003; 2005; 2005; 2006; 2007] or by applying an additional drain-source voltage and measuring the displacement currents at the, source contact and at the drain contact independently and simultaneously, which allow additional insight into the individual potential drops at the various interfaces of the device [Majima *et al*, 2007; Suzuki *et al*, 2008].

In the simplest and perhaps most intuitive DCM configuration, only one metal contact is fabricated and all charges are injected and extracted through this contact [Liang *et al*, 2009; Chang *et al*, 2010; 2011; Liang *et al*, 2011]. In addition, by using devices with very long channels ($L_{channel}$), the displacement currents and transit times can be made sufficiently long to obtain large signal-to-noise ratios during the measurements, and this configuration is termed as LCC devices [Liang *et al*, 2009].

In most previous reports of DCM on organic TFTs or LCC devices [Ogawa *et al*, 2005; Majima *et al*, 2007; Suzuki *et al*, 2008; Liang *et al*, 2009; Chang *et al*, 2010; 2011; Liang *et al*, 2011], the measurements were performed on devices based on the same organic semiconductor (pentacene), making it difficult to draw conclusions regarding the influence of the choice of the semiconductor on the trapping dynamics. In a few cases [Ogawa *et al*, 2003; Ogawa, 2005; Ogawa *et al*, 2006; 2007], DCM results obtained from pentacene TFTs were compared with results from poly(3-hexylthiophene) (P3HT) [Ogawa, 2005; Ogawa *et al*, 2006] or C_{60} TFTs [Ogawa *et al*, 2003; 2007], but the performance of the latter devices was relatively poor; the P3HT TFTs had a very low carrier mobility (10^{-4} cm^2/Vs), and the response of the C_{60} TFTs was severely degraded by the ambient air. One report showed DCM results obtained from a tetracene single-crystal FET [Xia *et al*, 2007], but again, no comparison with other semiconductors was provided. Therefore, to investigate how the trapping behavior probed by the DCM method is influenced by the choice of the organic semiconductor, LCC devices were fabricated and characterized.

One of the questions to be addressed with this experiment is whether these differences in the observed carrier mobilities are reflected in the density of trapped charges that is probed by the DCM techique. In addition to using four different semiconductors, four different contact metals [gold (Au), silver (Ag), copper (Cu), and palladium (Pd)] were employed in order to investigate whether the choice of the contact metal has an influence on the trapping behavior. In pentacene LCCs, a significantly smaller density of trapped charges was observed when Cu, as opposed to Au, was used as the contact metal [Liang *et al*, 2011].

5.3 DEVICE FABRICATION

The structure and fabrication process of LCC devices are discussed in the following Subsections. To compare the field-effect mobilities extracted from DCM technique and device characterization of TFT devices, the organic TFTs were fabricated using similar dielectric and

semiconductor; as for LCC devices. The fabrication process of these TFTs is given in Section 5.3.2.

5.3.1 Long-Channel Capacitor

The schematic cross-section and the layout of the LCC devices are given in Figure 5.1. This structure looks like a structure of FET with either source or drain contacts removed. The LCC device consists of a gate metal contact, gate dielectric, organic semiconductor, and a top metal contact.

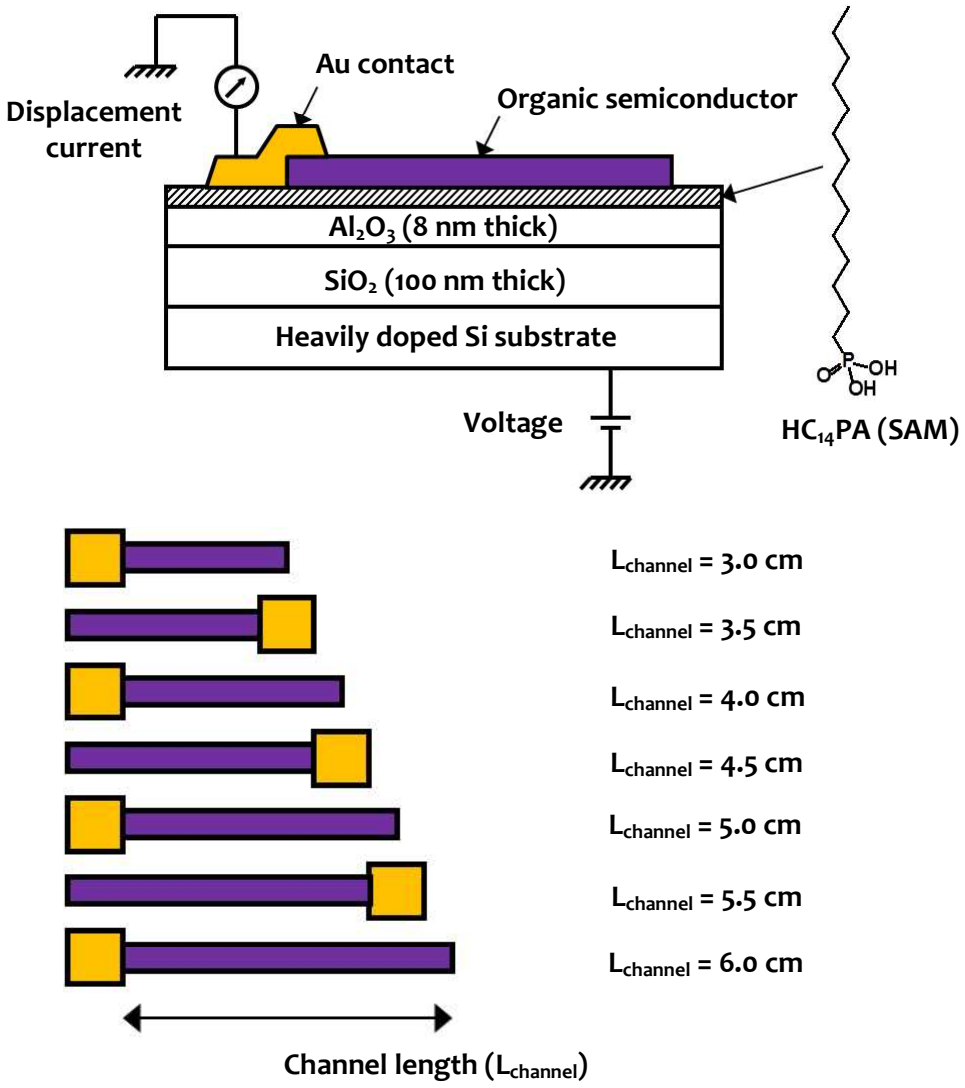

Figure 5.1 : Schematic Diagram showing the Cross-section and Layout of the Long-channel Capacitors

The step-by-step process flow for fabricating LCC devices is shown schematically in Figure 5.2. The LCC devices were fabricated on heavily doped silicon substrates, with the substrate also serving as the gate electrode. The gate dielectric is a combination of a 100-nm-thick layer of silicon dioxide (grown by dry thermal oxidation), an 8-nm-thick layer of aluminum oxide (deposited by ALD), and a 1.7-nm-thick SAM of HC_{14}-PA; obtained by immersing the substrate into a 2-propanol solution of the phosphonic acid). The total thickness of the SiO_2/Al_2O_3/SAM gate dielectric is 110 nm, and it has a capacitance per unit area of 34 nF/cm^2 [Hofmockel *et al*,

2013]. Onto this gate dielectric, a 25-nm-thick layer of the organic semiconductor was deposited in vacuum through a shadow mask, so that seven LCCs with a channel width of 0.3 cm and with channel lengths ranging from 3 to 6 cm (*i.e.*, with channel areas ranging from 0.9 to 1.8 cm^2) were obtained on each substrate. During the semiconductor depositions, the substrates were held at a temperature of 60 to 80 °C, depending on the semiconductor (see Table 3.1). The chemical structures of the four semiconductors, pentacene, DNTT, C_{10}-DNTT and DPh-DNTT, are already shown in Figure 3.3.

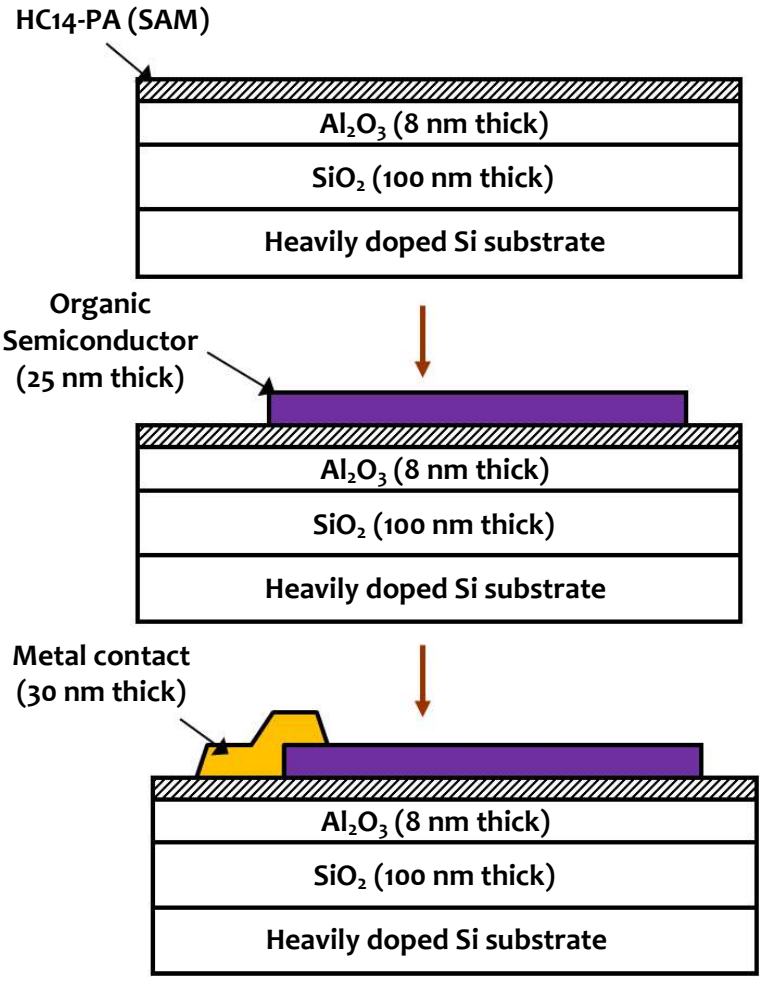

Figure 5.2 : Schematic Structure showing the Step-by-step Fabrication of Long-channel Capacitor Devices

The LCCs were completed by depositing a 30-nm-thick metal contact (Au, Ag, Cu or Pd) near one end of each LCC by thermal evaporation in vacuum through another shadow mask. The metal contacts have an area of 0.5 cm^2 and form a small overlap area with the organic semiconductor layer. The DCM technique was performed using an Agilent 4156C Semiconductor Parameter Analyzer, with one source-measure unit (SMU) connected to the gate electrode to apply the voltage and a second SMU connected to the metal contact to measure the displacement current.

5.3.2 Thin-Film Transistor

The schematic cross-section of the organic TFTs fabricated on rigid silicon substrates is shown in Figure 5.3. These devices consist of heavily doped p-type silicon wafer as the substrate and gate electrode; combination of 100 nm-thick SiO_2 (by dry thermal oxidation), 8 nm-thick

Al_2O_3 (by ALD), and 1.7 nm-thick HC_{14}-PA SAM (by immersing the substrate in the solution of HC_{14}-PA SAM in 2-propanol solution) as the gate dielectric; 25 nm-thick organic semiconductor (by vacuum evaporation); and 30 nm-thick gold source and drain contacts (by vacuum evaporation). The hole-transport organic semiconductors *i.e.* pentacene, DNTT, C_{10}-DNTT and DPh-DNTT were used for fabrication of p-channel TFTs. The fabricated organic TFT have L of 100 µm and W of 200 µm. The gate dielectric capacitance per unit area in these TFTs was characterized to be 34 nF/cm² [Hofmockel *et al*, 2013].

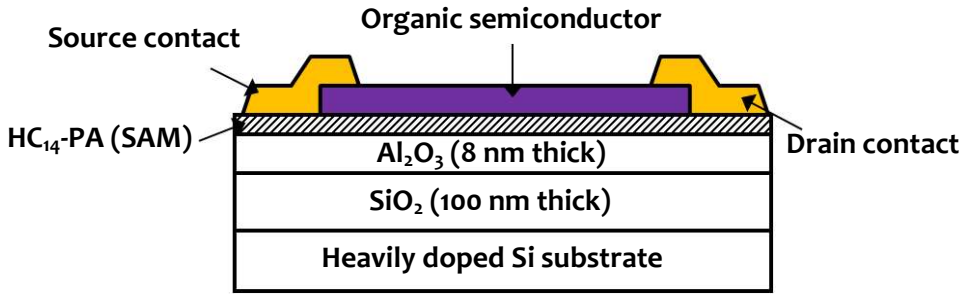

Figure 5.3 : Schematic Diagram showing the Cross-section of the Organic TFTs Fabricated on Rigid Silicon Substrates

5.4 RESULTS AND DISCUSSIONS

All measurements were carried out in ambient air at room temperature and without encapsulation of the devices. The results obtained from DCM technique and those obtained from TFT device characteristics are discussed here.

5.4.1 General Considerations for DCM

Figure 5.4(a) depicts the waveform of the voltage applied between the gate electrode and the metal contact during the DCM technique, with the metal contact held at ground potential. The voltage was first ramped from +40 V to -40 V and then back from -40 V to +40 V, always with a constant rate of 1.5 V/s. Figure 5.4(b) shows the displacement current measured at the metal contact as a function of the applied voltage; this particular measurement was performed on an LCC with a channel area of 1.8 cm² (channel length of 6 cm) and with DNTT as the semiconductor and Au as the contact metal.

As can be seen, when the applied voltage is ramped from +40 V towards more negative values (forward sweep), the displacement current initially has a small, constant, positive value. In this regime, the semiconductor is devoid of mobile charges (*i.e.*, there is no accumulation channel), so changing the applied voltage affects only the amount of charge on the capacitance formed by the geometric overlap between the metal contact and the gate electrode, and so the displacement current in this regime (below the threshold voltage V_{th}) is determined solely by the capacitance formed between the metal contact and the gate electrode [Liang *et al*, 2009],

$$I_{below-Vth} = \frac{\partial Q_{contact}}{\partial t} = -C_{contact}\frac{\partial V}{\partial t} = -A_{contact}C_{diel}\frac{\partial V}{\partial t} \quad (5.1)$$

where $Q_{contact}$ is the charge flowing into or out of the region underneath the metal contact, t is the time, $C_{contact}$ is the capacitance formed between the metal contact and the gate electrode, $\partial V/\partial t$ is the voltage sweep rate (1.5 V/s), $A_{contact}$ is the area of the metal contact (0.5 cm²), and C_{diel} is the gate-dielectric capacitance per unit area (34 nF/cm²).

It is important to note that changing the applied voltage towards more negative (positive) values produces a positive (negative) displacement current, due to the fact that the potential change acts on the gate electrode, while the displacement current was measured at the metal contact. According to Eq.(5.1), the displacement current in the regime in which the semiconductor is devoid of mobile charges should be about 25 nA. According to Figure 5.4, the displacement current actually measured in this regime is about 1 nA. The reason for the discrepancy between the calculated and measured values is not known.

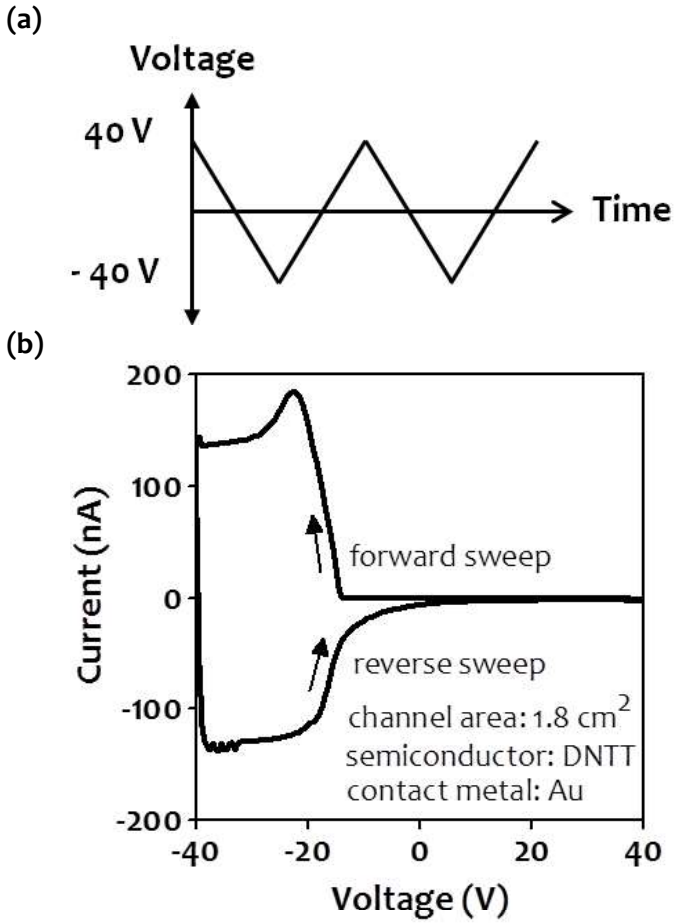

Figure 5.4 :(a) Waveform of the Voltage Applied between the Gate Electrode and the Metal Contact of the LCC Devices, and (b) Displacement Current Measured on an LCC with a Channel Area of 1.8 cm^2 and with DNTT as the Semiconductor and Au as the Contact Metal

When the applied voltage reaches the threshold voltage (-14 V), a sharp increase in the measured displacement current indicates the sudden injection of a large number of positive charges from the metal contact into the semiconductor. These charges spread across the entire semiconductor area and form an accumulation channel near the semiconductor/dielectric interface that balances the negative charge on the gate electrode (more precisely, the portion of the gate charge that is not already balanced by fixed or trapped charges in the gate dielectric or at the interface). The formation of this accumulation channel requires that the injected charges are transported from the metal contact in a lateral direction parallel to the dielectric interface towards the end of the semiconductor region, so the time required to complete the formation of the channel (and hence the slope of the leading edge of the peak observed in the measured

displacement-current *vs.* gate-voltage curve) depends on the charge-carrier mobility and on the channel length ($L_{channel}$ = 6 cm in this particular device) [Liang *et al*, 2009].

Once the formation of the accumulation channel is completed, the displacement current decreases to a constant, positive value that is determined by the total capacitance formed by combination of the metal contact and the accumulation channel on one side and the gate electrode on the other side [Liang *et al*, 2009],

$$I_{above-Vth} = \frac{\partial(Q_{contact}+Q_{channel})}{\partial t} = -(A_{contact} + A_{channel})C_{diel}\frac{\partial V}{\partial t} \quad (5.2)$$

where $Q_{channel}$ is the charge flowing into or out of the channel to balance the voltage-dependent gate charge and $A_{channel}$ is the area of the semiconductor channel (1.8 cm^2 in this particular device). In this regime, any change of the applied voltage will change the amount of charge in the accumulation channel, and since the area of the channel is much larger than the area of the metal contact ($A_{channel}$>$A_{contact}$), the displacement current in this regime will be much larger than the displacement current measured below the threshold voltage. According to Eq.(5.2), the displacement current in the above-threshold regime should be about 120 nA, and according to Figure 5.4, the displacement current actually measured in this regime is about 140 nA, in reasonable agreement with the calculated value.

When the applied voltage was ramped back from -40 V towards more positive values (reverse sweep), the amount of negative gate charge is monotonically decreased and thus the number of positive charges in the channel also decreases monotonically, which means that excess positive charges are extracted from the semiconductor through the metal contact. Thus, the displacement current in this regime is negative, but provided the voltage ramp rate has the same magnitude as during the forward sweep (which is the case here), the magnitude of the displacement current is also the same as during the forward sweep, as given by Eq.(5.2). Once the voltage applied during the reverse sweep reaches the threshold voltage (-14 V), the accumulation channel disappears, and the device capacitance is reduced to the capacitance of the metal contact, and thus the magnitude of the displacement current decreases and eventually reaches a small, constant, negative value, given by Eq.(5.1).

There are two aspects in which the shape of the displacement-current *vs.* gate-voltage curve measured during the reverse sweep differs from that measured during the forward sweep: One is that the annihilation of the accumulation channel does not produce a sharp peak in the displacement current, as was the case during the formation of the accumulation channel during the forward sweep. The other is that the drop in the displacement current upon annihilation of the accumulation channel during the reverse sweep is less abrupt and more gradual than the increase in the displacement current upon formation of the accumulation channel during the forward sweep. This gradual decrease of the displacement current in the reverse sweep is due to the delayed emission of trapped charges during or following the annihilation of the channel [Liang *et al*, 2009; Chang *et al*, 2010].

By integrating the measured displacement current over the applied voltage and multiplying with the inverse of the voltage sweep rate, the number of charges injected into the semiconductor during the forward sweep ($N_{injected}$) and the number of charges extracted from the semiconductor during the reverse sweep ($N_{extracted}$) can be calculated [Liang *et al*, 2009],

$$N_{injected} = \left|\frac{1}{q}\left(\frac{\partial V}{\partial t}\right)^{-1}\int_{V_{start}}^{V_{end}}(I_{forward} - I_{below-Vth})dV\right| \quad (5.3)$$

$$N_{extracted} = \left|\frac{1}{q}\left(\frac{\partial V}{\partial t}\right)^{-1}\int_{V_{end}}^{V_{start}}(I_{reverse} - I_{below-Vth})dV\right| \quad (5.4)$$

where q is the electronic charge, $\partial V / \partial t$ is the voltage sweep rate, V_{start} and V_{end} are the voltages at the beginning and the end of the forward and reverse sweeps (V_{start} = +40 V; V_{end} = -40 V), $I_{forward}$ and $I_{reverse}$ are the displacement currents measured during the forward and reverse sweep, and $I_{below\text{-}Vth}$ is the displacement current measured below the threshold voltage in the absence of an accumulation channel.

By subtracting the number of charges extracted from the semiconductor during the reverse sweep ($N_{extracted}$) from the number of charges injected into the semiconductor during the forward sweep ($N_{injected}$), the number of charges being trapped in the device during the forward and reverse sweep ($N_{trapped}$) can be calculated [Liang *et al*, 2009],

$$N_{trapped} = N_{injected} - N_{extracted} \tag{5.5}$$

Since the number of charges being trapped during the measurement is expected to depend not only on the material properties, but also on the device geometry, it is useful to normalize $N_{trapped}$ with respect to the device geometry. Figure 5.5 summarizes the results of DCM performed on LCCs in which the channel length was varied from 3 cm to 6 cm, which means that the area of the organic semiconductor varied from 0.9 cm² to 1.8 cm².

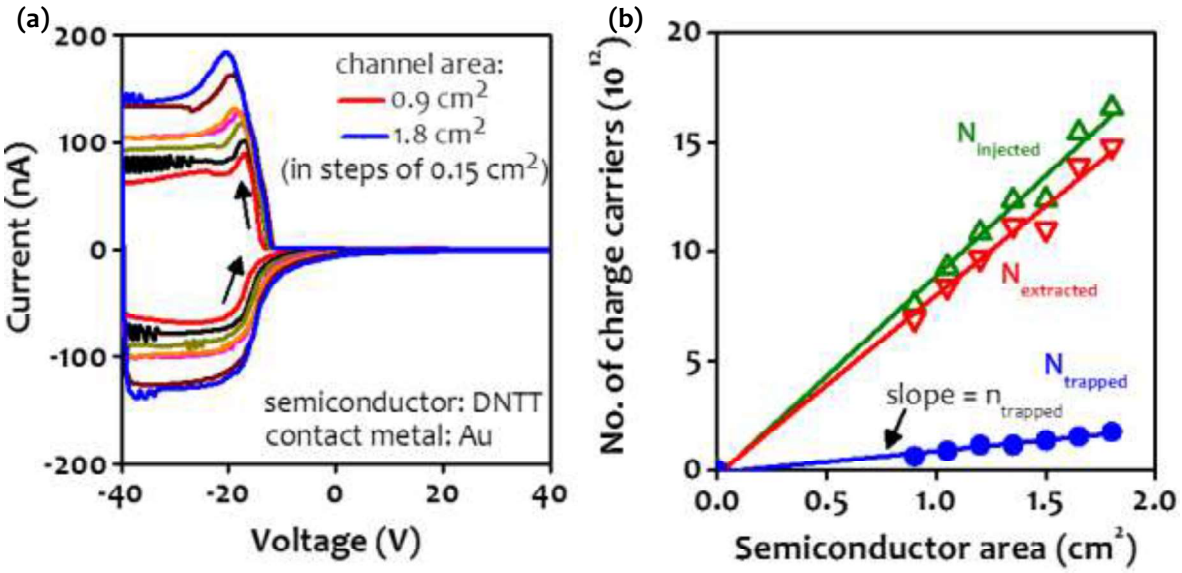

Figure 5.5 :(a) Displacement Currents Measured on LCC devices with Semiconductor Areas Ranging from 0.9 cm² to 1.8 cm²; All Curves from the First Sweep, (b) Number of Charges Injected during the Forward Sweep, Extracted during the Reverse Sweep, and Trapped during Forward and Reverse Sweep as a function of the Semiconductor Area; All Three Parameters Increase approximately Linearly with the Semiconductor Area

In Figure 5.5(a) it can be seen that the magnitude of the displacement current measured below the threshold voltage is independent of the semiconductor area, which is in agreement with the fact that the displacement current in this regime is determined only by the overlap area between the metal contact and the gate electrode, not by the area of the semiconductor; see Eq.(5.1). In contrast, the magnitude of the displacement current measured above the threshold voltage shows a monotonic dependence on the semiconductor area, which is in agreement with Eq.(5.2).

In Figure 5.5(b), the numbers of injected, extracted and trapped charges calculated using Eq.(5.3), (5.4) and (5.5) are plotted as a function of the semiconductor area. As can be seen, all three parameters increase approximately linearly with the semiconductor area, indicating that the charge distribution across the semiconductor area is approximately homogeneous. It is therefore reasonable to normalize the number of trapped charges ($N_{trapped}$) with respect to the area of the organic semiconductor ($A_{channel}$) and define an effective density of trapped charges ($n_{trapped}$),

$$n_{trapped} = {}^{N_{trapped}}\!/_{A_{channel}} \tag{5.6}$$

It can be concluded that the number of charge-carriers injected into semiconductor, extracted out of semiconductor, and trapped during the injection and extraction of charge-carriers are distributed uniformly over the entire semiconductor area; and density of charge-carriers, which are trapped is independent of the area of semiconductor.

5.4.2 Effect of Successive Sweeps during DCM

Figure 5.6 shows the DCM results on an LCC with a channel area of 1.8 cm^2, with DNTT as organic semiconductor and Au as the metal contact. The influence of the successive sweeps on the injection, extraction and trapped number of charge-carriers, along with the variation in threshold voltage and trapped carrier density, are summarized in various graphs of Figure 5.6. The effect of repeating the measurements (a total of nine successive sweeps) on measured displacement current as a function of the applied voltage is given in Figure 5.6(a). This graph shows that with successive sweeps the curve is shifting more towards the direction of the applied voltage (*i.e.* in the direction of more negative voltage) and the amount of shift is maximum from 1st sweep to 2nd sweep, however, it reduces drastically with successive sweeps.

The threshold voltage estimated from the onset of the peak in the displacement current measured during the forward sweep shifts by a few volts towards more negative values (see also Figure 5.6(b)). This shift of the threshold voltage during repeated measurements was also observed by Liang *et al* [Liang *et al*, 2009; 2011] and was ascribed to the filling of more and more deep trap states during each measurement.

Charges trapped in deep states remain inside the device after the completion of the measurement and affect the threshold voltage observed during the following measurement. As more and more deep states are filled, the density of deep states available in the device is expected to decrease with each measurement. Indeed for the present measurements, using Eq.(5.3), (5.4) (5.5) and (5.6) the density of charges trapped during each measurement is found to decrease from 10^{12} cm^{-2} during the first measurement to 3×10^{11} cm^{-2} during the ninth measurement. The same can be seen in Figure 5.6(c and d). These values are larger by an order of magnitude than those reported by Liang *et al* [Liang *et al*, 2009], but it should be noted that in present measurements the gate-induced charge density is about two times larger and the duration of each measurement is about four times longer than in the measurements reported by Liang *et al*, and both of these parameters are likely to affect the trapping probability.

Assuming that all charges trapped during a particular measurement are still in deep states at the beginning of the following measurement, the threshold-voltage shift expected to be induced by these trapped charges can be calculated as follows,

$$\Delta V_{th} = {}^{q.\,n_{trapped}}\!/_{C_{diel}} \tag{5.7}$$

However, the measured threshold-voltage shifts are on average a factor of two to three smaller than the threshold-voltage shifts calculated using Eq.(5.7). For example, the density of

charges trapped during the first measurement is 1×10^{12} cm^{-2}, which, according to Eq.(5.7), would be expected to induce a threshold-voltage shift of 4.6 V, but the measured shift from the first to the second measurement is only 2.3 V. This indicates that approximately one half to two thirds of the charges trapped during each measurement are released before the beginning of the following measurement, which suggests that some of the traps have characteristic lifetimes that are shorter than the duration of a single measurement.

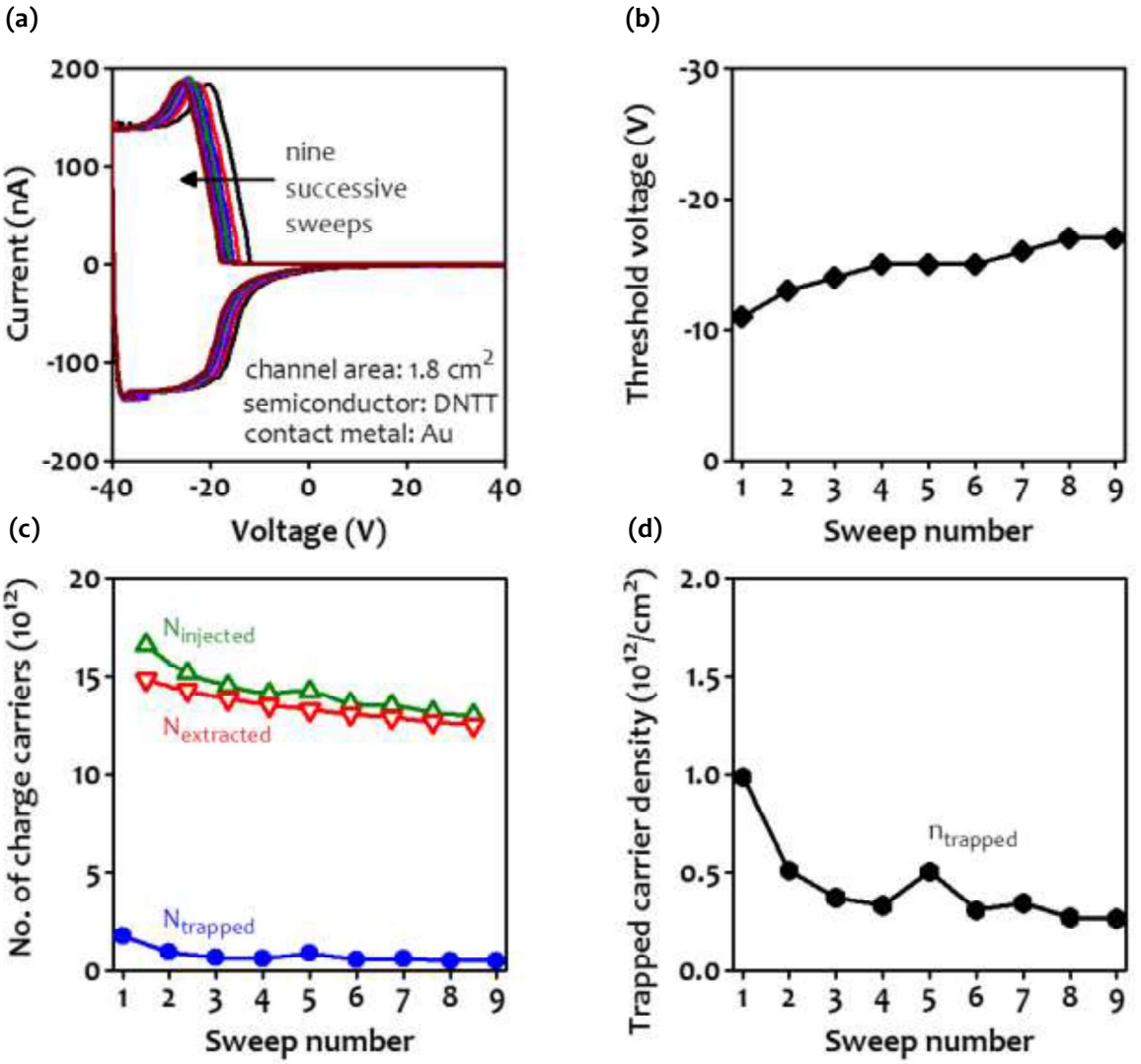

Figure 5.6 :(a) Displacement Current Measured during 9 Successive Forward and Reverse Sweeps, (b) Threshold Voltage Estimated from the Onset of the Peak in the Displacement Current Measured during the Forward Sweep of 9 Successive Measurements, (c) Number of Injected, Extracted and Trapped Charges during each of 9 Successive Measurements, and (d) Density of Trapped Charges during each of 9 Successive Measurements

5.4.3 Choice of the Semiconductor

To see how the density of trapped charges probed by the DCM is influenced by the choice of the organic semiconductor, LCCs based on four different small-molecule semiconductors: pentacene, DNTT, C_{10}-DNTT, and DPh-DNTT were fabricated. All of these semiconductors have previously demonstrated great promise for the realization of organic p-channel TFTs with

good static and dynamic performance and stability on flexible plastic substrates [Myny *et al*, 2011; Zschieschang *et al*, 2011; Zschieschang *et al*, 2012; Głowacki *et al*, 2013; Yokota *et al*, 2013; Zaki *et al*, 2013; Zschieschang *et al*, 2013; Bisoyi *et al*, 2014], but they have notably different carrier mobilities, ranging from 1 cm^2/Vs (pentacene) to 7 cm^2/Vs (DPh-DNTT). One of the questions to be addressed with this experiment is whether these differences in the observed carrier mobilities are reflected in the density of trapped charges that is probed by the DCM technique.

The DCM results *i.e.* the influence on the injection, extraction, and trapping of charge-carrier dynamics by using four different organic semiconductors are summarized in Figure 5.7. Figure 5.7(a) shows the displacement-current *vs.* gate-voltage curves measured on LCCs based on all four semiconductors, all with a channel area of 1.5 cm^2 and with Au as the contact metal. According to Eq.(5.1) and Eq.(5.2), the displacement currents measured well below and well above the threshold voltage are expected to be independent of the choice of the semiconductor, and indeed they are very similar in all four curves. In contrast, the displacement current measured in the transition regions near the threshold voltage, both in the forward and in the reverse sweep, is expected to be greatly affected by the carrier mobility and by the trapping dynamics [Liang *et al*, 2009]. Indeed, in the transition regions small differences between the four curves can be discerned.

Using Eq.(5.3), (5.4), (5.5) and (5.6), number of charges injected and extracted during the forward and reverse sweeps ($N_{injected}$, $N_{extracted}$) and the number and the density of charges trapped during the DCM ($N_{trapped}$, $n_{trapped}$) are calculated. In Figure 5.7(b and c), the values calculated for $N_{injected}$, $N_{extracted}$ and $n_{trapped}$ are plotted *versus* the carrier mobility. The carrier mobility is estimated from the slope of the peak (μ_{DCM}) of displacement current associated with the formation of the accumulation channel during the forward sweep [Liang *et al*, 2009].

As can be seen, $N_{injected}$, $N_{extracted}$ and $n_{trapped}$ are all very similar for the four semiconductors, despite the significant differences in carrier mobility. In particular, no systematic trend between the density of trapped charges and the carrier mobility can be discerned. This is somewhat surprising, considering that it is commonly believed that the charge-carrier mobility in organic semiconductors is at least to some extent limited by charge-carrier trapping. A possible explanation is that the differences between the charge-carrier mobilities in the four semiconductors are caused by trapping events that have characteristic lifetimes which are shorter than the duration obtained from DCM, so that these trapping events remain undetected by these measurements (in other words, the carriers are released from the traps before the end of the measurement). This explanation is in line with the observation that the charge-carrier mobility in organic semiconductors is limited mainly by shallow traps, *i.e.*, by traps that have small activation energies and hence short characteristic lifetimes [Li *et al*, 2014] (as opposed to bias-stress-induced threshold-voltage shifts, which are more likely to be caused by trapping in deep states with long characteristic lifetimes [Sirringhaus, 2009; Bobbert *et al*, 2012]). An alternative explanation is that the differences in carrier mobility are not primarily due to differences in the density of charges being trapped, but due to secondary effects resulting from the trapping events (*e.g.*, differences in the scattering cross-sections of the filled trap states depending on the trap energy), or due to effects that are not at all related to charge-carrier trapping, but perhaps to differences in the transfer integrals or reorganization energies of the molecules [Cornil *et al*, 2001; Troisi and Orlandi, 2005; Coropceanu *et al*, 2009; Sánchez-Carrera *et al*, 2010] or to charge-carrier scattering induced by structural or energetic disorder.

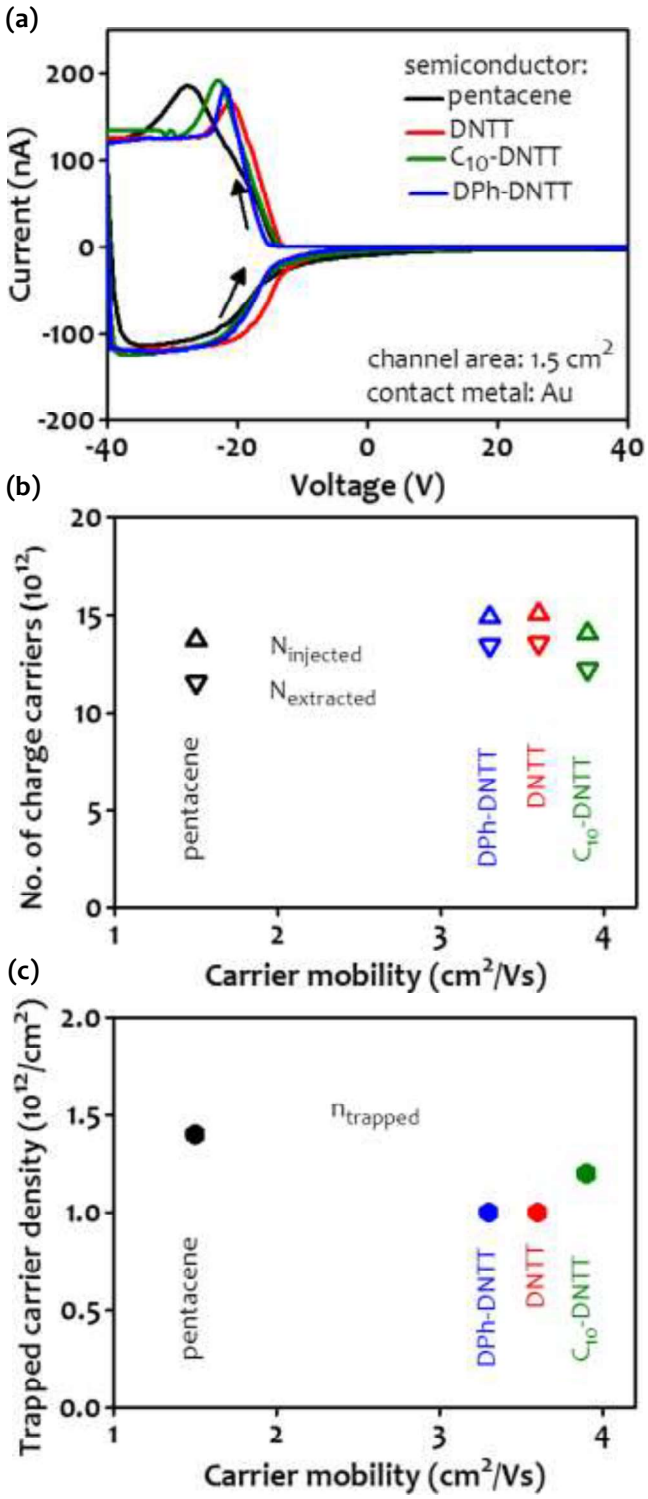

Figure 5.7 : (a) Displacement Current Measured on LCCs based on all Four Semiconductors, All with a Channel Area of 1.5 cm^2 and with Au as the Contact Metal; All Curves from the First Sweep, (b) Number of Charges Injected during the Forward Sweep and Extracted during the Reverse Sweep Plotted *versus* the Charge-carrier Mobility Estimated from the Displacement Current Measurements [Liang *et al*, 2009], (c) Density of Charges Trapped during the Displacement Current Measurement Plotted *versus* the Charge-carrier Mobility Estimated from the Displacement Current Measurements

5.4.4 Choice of the Contact Metal

Figure 5.8(a) shows the displacement-current *vs.* gate-voltage curves measured on DNTT-based LCCs with a channel area of 1.8 cm^2 and with either Au, Cu, Ag or Pd as the contact metal.

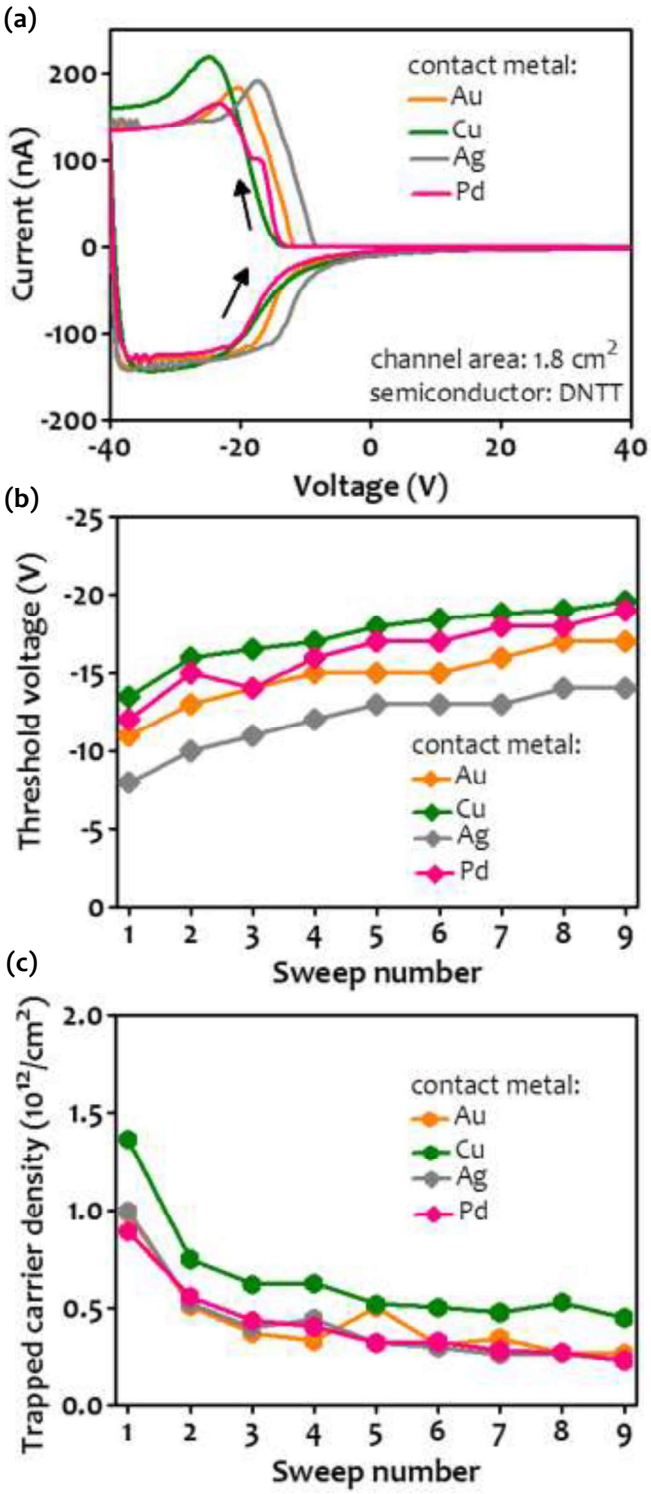

Figure 5.8 :(a) Displacement Current Measured on LCCs based on Au, Cu, Ag and Pd as the Contact Metal, all with DNTT as the Semiconductor and all with a Channel Area of 1.8 cm^2; All Curves from the First Sweep, (b) Calculated Threshold Voltage from DCM, (c) Density of Trapped Charges during 9 Successive Measurements

For this experiment, LCCs using DNTT as the semiconductor and gold, copper, silver or palladium as the contact metal, which have different barriers between HOMO level of organic semiconductor and metal work function were fabricated and characterized. In a similar experiment (using pentacene as the semiconductor), it was found that the density of trapped charges is significantly smaller in LCCs with Cu, as opposed to Au, as the contact metal [Liang *et al*, 2011]. Also, several other authors, have reported that the contact resistance of pentacene TFTs is smaller when Cu, rather than Au, is employed as the contact metal, while some authors have reported slightly smaller contact resistances for pentacene TFTs with Au, rather than Pd, as the contact metal [Wang *et al*, 2007; Necliudov *et al*, 2003].

The reason to choose DNTT for current study, rather than pentacene, as the semiconductor for the experiment is that DNTT TFTs provide larger field-effect mobility and better air stability compared with pentacene TFTs [Zschieschang *et al*, 2011]. DNTT TFTs are usually fabricated using Au as the contact metal, although Ag (deposited by inkjet-printing [Yokota *et al*, 2011], screen-printing [Peng and Chan, 2014] or vacuum deposition [Ren and Chan, 2014]) has also been successfully employed. Cu and Pd have not been previously employed as the contact metal for DNTT devices.

The measured displacement current results, showing the influence of the charge-carrier dynamics by using four different metal contacts (Au, Cu, Ag, Pd) with work function in a range of 4.26 eV to 5.6 eV and DNTT as organic semiconductor (HOMO energy level of 5.44 eV and energy gap of 3 eV), for channel area of 1.5 cm^2 is summarized in Figure 5.8. The main difference between the curves is the threshold voltage, which varies from -8 V for Ag to -11 V for Au, -12 V for Pd and -13 V for Cu (see also Figure 5.8(b)). The density of charges trapped during each of 9 successive DCM performed on LCCs based on all four contact metals is given in Figure 5.8(c). It appears that the choice of the contact metal has only a small influence on the density of trapped charges probed by the DCM; if anything, the density of trapped charges appears to be slightly larger for Cu than for Au, which is in contrast to the trend reported by Liang *et al* [Liang *et al*, 2011], although it should be pointed out again that Liang *et al* employed pentacene, rather than DNTT, as the semiconductor.

5.4.5 TFT Characterization

The transfer and output characteristics of pentacene, DNTT, C_{10}-DNTT and DPh-DNTT based TFTs on rigid silicon substrates are given in Figure 5.9. For output characteristics, the drain current was measured as a function of continuous change in drain-source voltage from 0 V to -30 V at specified gate-source voltages of -10 V, -15 V, -20 V, -25 V and -30 V. The transfer characteristics are plotted for continuous change in gate-source voltage (V_{GS}) from 0 V to -30 V at a specified drain-source voltage (V_{DS}) of -30 V. The output characteristics of all the TFT show nice linear and saturation behavior.

The extracted field-effect mobilities and threshold voltage of pentacene, DNTT, C_{10}-DNTT, and DPh-DNTT on rigid silicon substrates are 1.0 cm^2/Vs and -12 V, 4.0 cm^2/Vs and -12 V, 6.5 cm^2/Vs and -7.0 V, and 7.0 cm^2/Vs and -10 V, respectively. These devices show low gate leakage current *i.e.* below 10^{-10} A. The current on/off ratio are 10^7, 10^8, 10^8, 10^7 for pentacene, DNTT, C_{10}-DNTT, and DPh-DNTT based TFTs, respectively. The threshold voltage V_{th} (estimated from the onset of the peak associated with the formation of the accumulation channel during the forward sweep during DCM), the carrier mobility estimated from the slope of that peak (μ_{DCM}) during DCM measurements [Liang *et al*, 2009]; and the carrier mobility and threshold voltage calculated from current-voltage measurements performed on TFTs (μ_{TFT}) based on the same semiconductors and fabricated on the same type of substrate ($Si/SiO_2/Al_2O_3$/SAM) with the same film thicknesses and also using a top-contact device structure [Hofmockel *et al*, 2013] are given in Table 5.1.

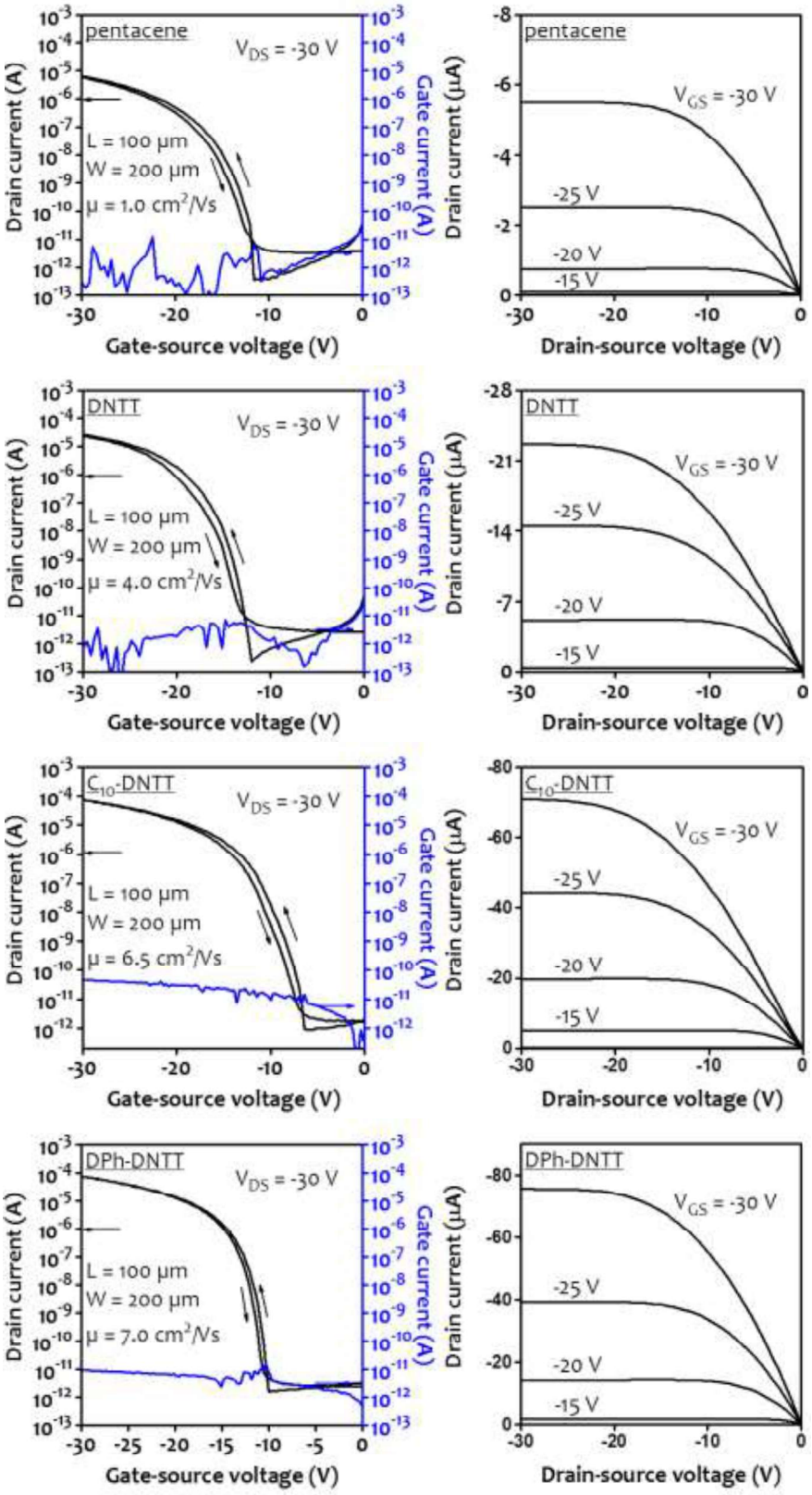

Figure 5.9 : Transfer and Output Characteristics of Pentacene, DNTT, C_{10}-DNTT, and DPh-DNTT based TFTs (from Top to Bottom) Fabricated on Rigid Silicon Substrates

Table 5.1 : Number of Injected, Extracted and Trapped Charges, Density of Trapped Charges, Threshold Voltage (V_{th}) and Charge-carrier Mobility (μ_{DCM}) Estimated from the Displacement Current Measurements, as well as Charge-carrier Mobility and Threshold Voltage Calculated from TFT Measurements (μ_{TFT})

Semiconductor	pentacene	DNTT	C_{10}-DNTT	DPh-DNTT
$N_{injected}(10^{12})$	13.7	15.0	14.1	15.0
$N_{extracted}(10^{12})$	11.6	13.5	12.2	13.4
$N_{trapped}$ (10^{12})	2.1	1.5	1.9	1.6
$n_{trapped}(10^{12}/cm^2)$	1.4	1.0	1.2	1.0
$V_{th,DCM}$ (V)	-13	-10	-13	-10
μ_{DCM} (cm^2/Vs)	1.5	3.6	3.9	3.3
$V_{th,TFT}$ (V)	-12	-12	-7.0	-10
μ_{TFT} (cm^2/Vs)	1.0	4.0	6.5	7.0

These field-effect mobility (μ_{DCM}) and threshold voltage ($V_{th,\ DCM}$) extracted using LCC device from the DCM measurements are comparable to the values of field-effect mobility (μ_{TFT}) and threshold voltage ($V_{th,\ TFT}$) obtained from device characteristics of TFTs.

5.5 CONCLUSIONS

The charge trapping dynamics in organic TFTs is understood by performing DCM on LCC devices based on four different organic semiconductors (pentacene, DNTT, C_{10}-DNTT and DPh-DNTT) and four different contact metals (Au, Ag, Cu, Pd). The fabrication process of LCC devices and organic TFTs on rigid Si substrates are discussed. From the measured displacement currents, the number of charges injected into and extracted from the semiconductor as well as the density of charges trapped in the device during each measurement have been calculated.

The displacement currents calculated for LCC devices consisting of DNTT as semiconductor and Au as metal contact, with channel area varying from 0.9 cm^2 to 1.8 cm^2 with the step of 0.15 cm^2, shows that the number of charge-carriers injected into semiconductor, extracted out of semiconductor, and trapped during the injection and extraction of charge-carriers are distributed uniformly over the entire semiconductor area; and density of charge-carriers, which are trapped is independent of the area of semiconductor.

The successive sweeps during DCM for LCC devices consisting of DNTT as semiconductor and Au as metal contact with a channel area of 1.8 cm^2, causes shift of threshold voltage (in the direction of more negative values during forward sweep) and the amount of shift is maximum from 1st sweep to 2nd sweep, however, it reduces drastically with successive sweeps. This shift in threshold voltage is due to the filling of deep trap states with each successive sweep.

The density of trapped charges probed by the DCM is very similar in all devices, despite the significant differences between the charge-carrier mobilities in the four semiconductors. A possible explanation for the lack of a systematic trend between the density of trapped charges and the charge-carrier mobility is that the mobilities are limited by trapping events that remain undetected by the DCM, perhaps due to significant differences in the trap energies. Another explanation is that the differences in mobility are due to effects other than charge-carrier trapping. Much like the choice of the semiconductor, the choice of the contact metal also does

not appear to have a significant effect on the trapping behavior except for a slightly larger density of trapped charges in devices with Cu contacts compared with devices with Au, Ag or Pd as the contact metal.

The field-effect mobility (μ_{DCM}) and threshold voltage ($V_{th,\ DCM}$) extracted using LCC device from the DCM measurements are comparable to the values of field-effect mobility (μ_{TFT}) and threshold voltage ($V_{th,\ TFT}$) obtained from device characteristics of TFTs.